Oscillatory Instabilities in a Rapidly Rotating Liquid Annulus

J. A. Szymczyk,* J. Siekmann,† and J. T. Cieśliński‡
University of Essen, Essen, Germany

Under low-gravity conditions, rotating fluid systems having liquid-solid, liquid-liquid, or liquid-gas interfaces with imposed (horizontal or vertical) temperature gradients are significantly influenced by thermal Marangoni effects. The flow within a rapidly rotating liquid cylinder with a free inner surface that is caused by a vertically applied temperature gradient is considered. The liquid-gas zone was heated from above and cooled from below. The onset of thermocapillary convection is investigated and the flow pattern at the interface as a function of the Marangoni number and the rotational speed for two liquids having different Prandtl numbers is analyzed. The topological flow structures are discussed in some detail.

Nomenclature

a = thermal diffusivity, m^2/s
Bo = Bond number—ratio of the centrifugal force to the surface tension force, $\rho_o \cdot \Omega^2 \cdot R^3/\sigma_o$
E = Ekman number—ratio of the viscous force to the Coriolis force in the liquid-gas zone, $\nu/\Omega \cdot R^2$
Fr = Froude number—ratio of the centrifugal force to the gravitational force, $\Omega^2 \cdot R/g$
g = acceleration due to gravity, m/s^2
H = height of the liquid-gas interface, m
Mg = Marangoni number—ratio of a force due to a surface tension gradient to the viscous force, $|\partial\sigma/\partial T| \cdot H \cdot \Delta T/(\mu \cdot a)$
Pr = Prandtl number—ratio of viscous diffusivity to thermal diffusivity, ν/a
R = radius, m
r = radial coordinate, m
T = temperature, K
Ta = Taylor number—ratio of the Coriolis force to the viscous force, $Ta^{1/2} = 2 \cdot \Omega \cdot H^2/\nu$
T_C = temperature of the cold wall, K
T_H = temperature of the hot wall, K
z = axial coordinate, m
ΔT = temperature difference, $T_H - T_C$, K
Θ = angular coordinate, rad
μ = dynamic viscosity, Ns/m^2
ν = kinematic viscosity, m^2/s
ρ_o = density, kg/m^3
σ = surface tension, N/m
Ω = angular velocity, rad/s

I. Background

A. Rotating Fluid Systems

CONVECTION in rotating fluids caused by an applied temperature gradient has been studied both experimentally and theoretically for a sufficiently wide range of the determining parameters. Without demanding completeness, Fig. 1 presents the representative works on convection and thermocapillary flow under rotation for different flow configurations and thermal conditions. One can differentiate four basic typi-

cal configurations: 1) horizontal fluid layers between two infinite plates (this case is of theoretical importance only)[1,2]; 2) liquid bridges, serving as simulated floating-zone configurations in crystal growth from the melt[3-5]; 3) containers completely filled with fluid having a free[6] or rigid surface[7] with insulated or perfectly conducting sidewalls[8] and different cross sections,[8] sometimes with an additional rotating lid[9]; and 4) annulus with solid outer and inner surfaces and different cross sections,[10,11] or with a rigid sidewall and free inner surface (so-called inverse liquid bridge).[12] In the case of a lack of a temperature gradient, fluid and container must rotate with the same constant angular velocity.

The rotating fluid system used in this investigation is shown in Fig. 2. It consisted of an annulus with a free inner liquid-air interface produced by the rotation of a transparent glass cell with a constant angular velocity. A cylindrical coordinate system (r, Θ, z) is used to describe this system, where the z axis coincides with the symmetry axis of the zone. The volume ratio for which the experiments have been conducted, i.e., $V_{fluid}/V_{chamber}$, was 0.5. The aspect ratio (altitude/diameter, H/D) was 1. The experimental chamber was rotated at various speeds of rotation, i.e., Ω = 62.83–104, 30 rad/s (600–1000 rpm).

The driving force for flows in this rotating cylindrical fluid system is the nonuniform temperature field. It produces variations of the fluid density and the surface tension at the fluid-fluid interface. As an effect of density variations, gravitational-buoyancy-driven motion occurs through the vertical gravitational force and centrifugal-buoyancy-driven motion produced by the radial centrifugal force. As an effect of surface tension variations, there results a thermocapillary convection. These three types of motion cannot be studied independently since they are closely coupled.

B. Linear Dynamics of Rotating Stratified Fluids

The flow in the rotating liquid-gas zone with a free inner surface is influenced by thermocapillary convection, gravitational and centrifugal buoyancy, and the motion of the solid container. Because of small Ekman numbers (herein, E is of the order 10^{-3}), the fluid motion with a free inner surface in the rotating cylinder is composed of four parts: a core motion, Ekman layers on the top and the bottom plates, a sidewall layer, and a side layer at the liquid-gas interface.

The dynamics of rotating fluids depends on stratification. For weak stratification, the fluid, in all regions, acts as if it were homogeneous, i.e., its interior dynamics is strongly controlled by the Ekman-layer suction. The Taylor-Proudman theorem is valid in the interior, and the sidewall layer[13,14] has a double structure and is made up of an inner Stewartson boundary layer of thickness $E^{1/3}$ in which viscous and Coriolis forces balance and an outer Stewartson $E^{1/4}$ layer,[15] which serves to match the fluid velocity to that of the vertical boundary layer. The thermocapillary flow at the liquid-gas interface

Rotating Fluid Systems
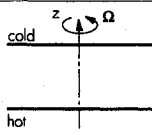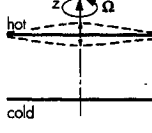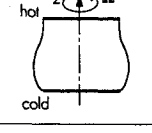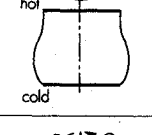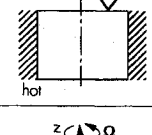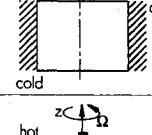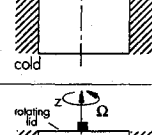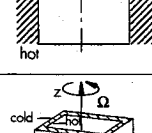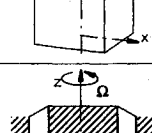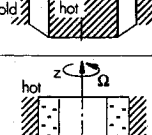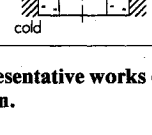
Author / Ref. Type of work	Geometry and thermal conditions	Objectives
Clever, Busse [1] Theoretical	cold ... hot	Steady finite amplitude. Two dimensional solutions for the problem of convection. Stability analysis.
Brown, Cheng [2] Theoretical	hot ... cold	Disturbance produced by an oscillating, shallow topographical feature in horizontal, relative motion. Explicit solution for a sinusoidal surface oscillation.
Smith [3] Theoretical	hot ... cold	Thermocapillary and centrifugal-buoyancy flow field for small Ekman number. Linear boundary-layer theory.
Chun, Wuest [4] Experimental	hot ... cold	Temperature oscillations. Single- or iso-rotation of both disks. Interaction of rotating flows with Marangoni convection.
Bubnov, Golitsyn [6] Experimental	hot	Convective structures in rotating vessels (rectangular other cylindrical) with and without lid. Wide range of Ra and Ta numbers.
Barcilon, Pedlosky [7] Theoretical	hot, $\dot{q}=0$, cold	Circulations produced by the resulting stratification. Solutions for conduction and convection dominated regimes.
Homsy, Hudson [8] Theoretical	hot, cold	Convection strongly influenced by centrifugal accelerations. Boundary-layer method. Side walls: perfectly conducting other insulated.
Lugt, Abbout [9] Theoretical	rotating lid, hot	Fluid circulation produced by a rotating lid. Monotonic or undulating with seperation bubbles streamline patterns. Incompressible homogeneous fluids.
Hunter [10] Theoretical	cold, hot	Axisymmetric flow for small Ta number. Upper surface rigid or free. Centrifugal forces negligible. Heat transfer purely conductive.
Busse, Or [11] Theoretical	cold, hot	Convection in annulus with conical end surface. Nonlinear equations. Thermal Rossby waves.
Szymczyk, Siekmann [12] Experimental	hot, cold	Flow regimes at the interface and in Fluid. Onset of thermocapillary convection and oscillations. Effect of rotation and Prandtl number.

Fig. 1   Representative works on convection and thermocapillary flow under rotation.

Fig. 2   Rotating liquid-gas cylinder with cylindrical coordinate system.

is confined to a thin boundary layer where the thermocapillary stress is balanced by viscous stresses. Moving away from the interface, viscous stresses cannot balance the resultant Coriolis forces, and so the int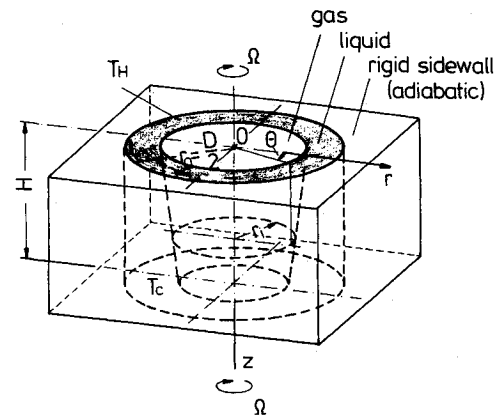erior of the cylinder remains in geo-strophical balance. This confinement of the thermocapillary convection to a boundary layer at the liquid-gas interface is a consequence of the Taylor-Proudman theorem for the motion in the inviscid core, since such a motion cannot vary in the z direction.

As the stratification increases, the dynamics in the interior is mainly controlled by Ekman-layer suction, but displays hybrid features; in particular, the dynamical fields can be decomposed into a homogeneous component, which satisfies the Taylor-Proudman theorem, and into a stratified component, which is baroclinic and satisfies a thermal wind relation. According to Ref. 13 the sidewall boundary layer exhibits a triple structure and is composed of 1) a buoyancy sublayer in which the viscous and buoyancy forces balance; 2) a hydrostatic baroclinic layer, where the buoyancy balances the vertical pressure gradient or Coriolis force[8]; and 3) a Stewartson $E^{\frac{1}{4}}$ layer. Stronger thermocapillary convection will cause a thickening of the domain of penetration, which is composed of the Marangoni boundary layer and several convection rolls away from the interface, and, possibly, an encroachment on the core as the temperature gradient is increased.

For strongly stratified fluids, the interior dynamics is found to be controlled by dissipative processes.[16] The Ekman layers will either turn out to be absent to a lowest order or to play only a purely passive role in the dynamics. (Whenever they are present, the structure of the Ekman layer is independent of the size of the stratification since the essential balance of forces, viz. Coriolis vs viscous, involves horizontal motions that are unaffected by the stratification.) The triple structure vertical boundary layer is replaced by a single layer of thickness $\mathcal{O}(E^{\frac{1}{2}})$. These drastic changes in the behavior of the fluid motion are intimately connected with the ability of the imposed stable stratification to inhibit vertical motion. If the temperature gradient is large enough, it is possible that the thermocapillary domain of penetration at the liquid-gas interface merges to the interior motion.

The experiments presented were conducted under weak and intermediate stratification conditions, such that the fluid behaved essentially as if it were homogeneous or the dynamics had a hybrid nature, exhibiting features of both homogeneous and stratified fluids. The main object of the present work, however, is the experimental investigation of the fluid dynamics at the liquid-gas interface.

II.   Experimental

The principal item of the experimental setup was the cylindrical experiment chamber made of glass (Fig. 3). This chamber contained the fluid system: liquid (silicone oil AK-0.65 or AK-5)/air. The liquid column was heated from above and cooled from below. Heating, cooling, and registration of the test data (temperature measurements with Pt-100) took place by means of sliding (contact) ring. In order to avoid mech-
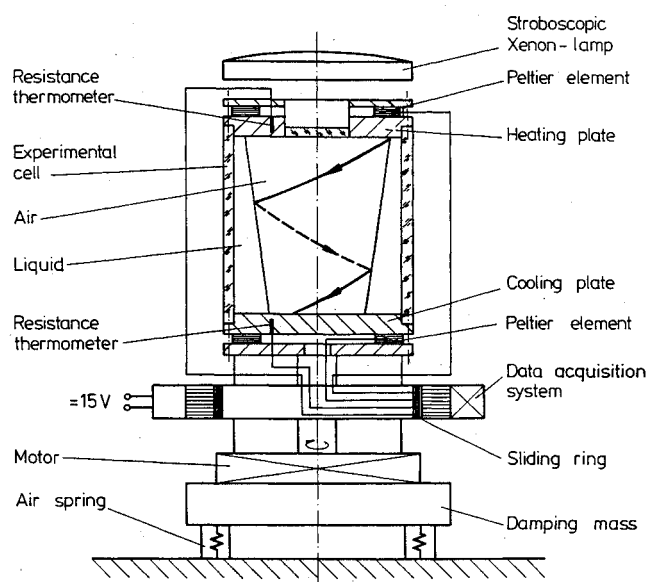
Fig. 3   Sketch of the experimental setup.

Fig. 4   Optical arrangement for flow visualization.

anical vibrations, two steps were undertaken: the revolving parts of the experimental stand were balanced statically and the experimental setup was housed on a damping mass, which was additionally located on air springs. For the purpose of flow visualization, a stroboscopic Xenon lamp was employed, together with settled out neutral-buoyant light scattering eccospheres serving as tracer particles (Fig. 4).

Pictures of the flow were taken with a camera. The exposure times were chosen in dependence on the flow pattern as short-
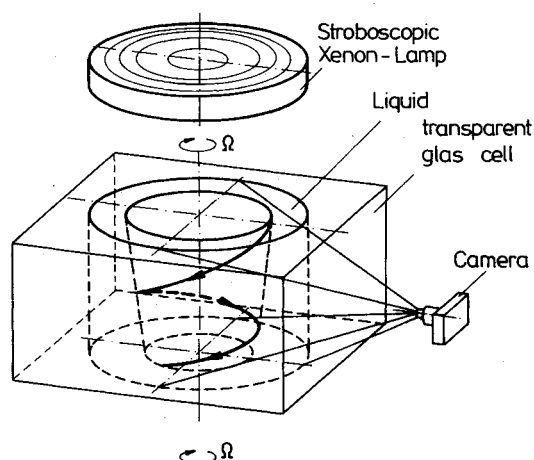
time exposure (0.5 s) or long-time exposure (2 s). By means of the optical arrangement (including a stroboscopic lamp), the rotating frame of reference was simulated accordingly, and, thus, each motion at the interface represents a relative motion of the liquid with respect to the rotating coordinate system. In reality, this motion is faster or slower than the rotational speed itself. The experimental procedure was as follows. First, the experiment chamber was rotated until the desired speed of rotation was achieved. Next, the temperature gradient directed parallel to the vertical cylindrical interface between liquid and air was established. Immediately after bringing about a temperature difference between the heated and cooled copper plates, thermocapillary convection was induced.
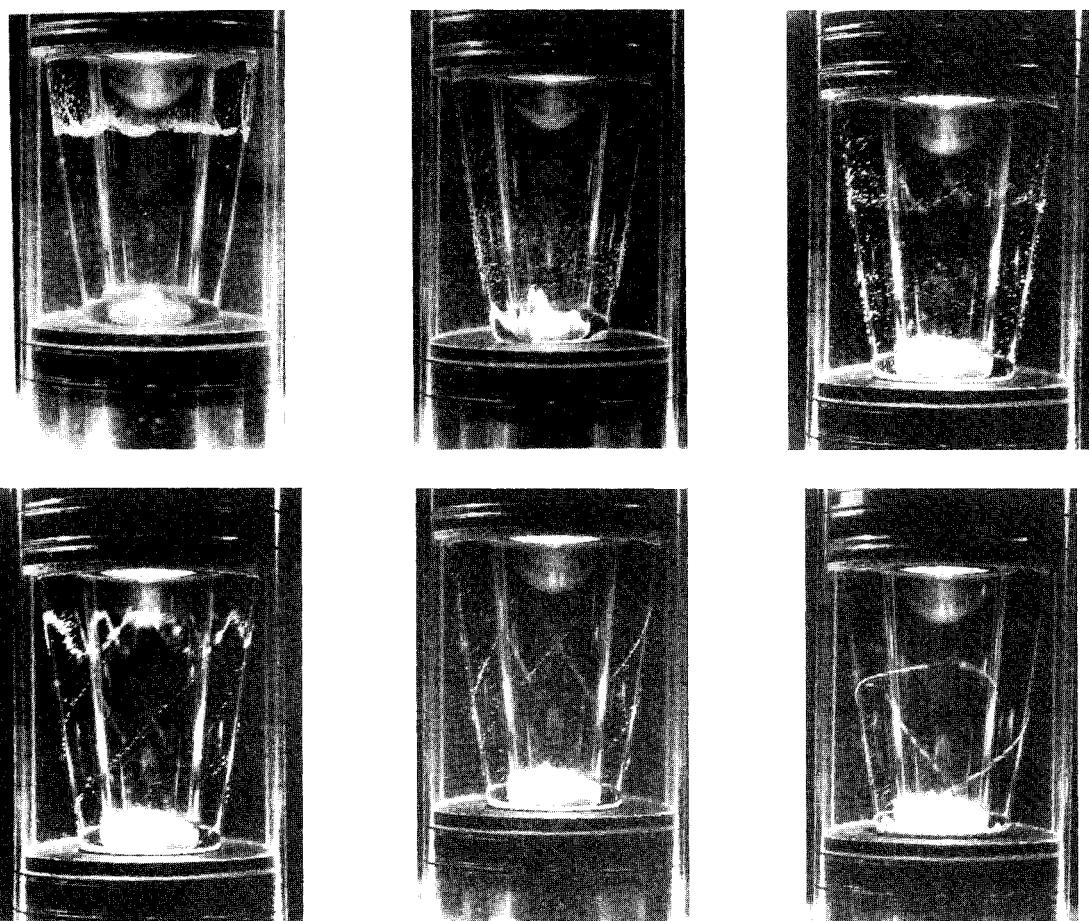

Fig. 5   Sequence of flow structures generated by an increasing temperature gradient in silicone oil AK-5: $Pr = 55$; $Fr = 8$; $\Omega = 62.83$ rad/s (600 rpm); $Ta = 1.97 \times 10^9$; $E = 4.51 \times 10^{-5}$.

III. Results

A. Flow Patterns

Figure 5 exhibits flow structures occurring at the interface at the constant speed of rotation $\Omega = 600$ rpm in a sequence generated by an increasing temperature gradient. Immediately after establishing a temperature difference between the upper and lower surface of the liquid-air zone, the interfacial convection is brought into action from above to below (first picture). Owing to rotation, the flow assumes the value of the circumferential component of the velocity (second picture), and next, by greater temperature gradients, develops first wave forms (third and fourth picture), and finally, helical structures in loop form (fifth and sixth picture).

According to the pictures taken and the observations made, four different flow regimes (modes) can be observed at the interface (Fig. 6): 1) slow laminar convection—the tracers move spirally at the interface (mode 1); 2) wave form (mode 2); 3) wave form and regular helical structure in loop form (mode 3); and 4) fast interfacial form. The tracers move directly from the top to the bottom of the experimental cell (mode 4). The second form, i.e., the wave form, can be interpreted as an
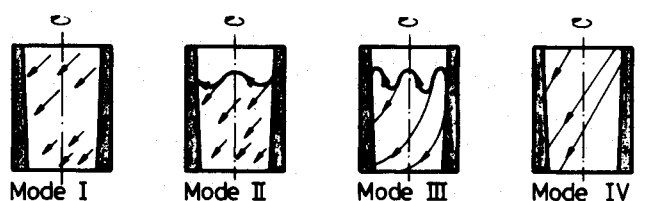
onset of oscillations. The third and the fourth modes are examples of oscillatory thermocapillary flows.

B. Development of the Thermocapillary Instability

The sequence of pictures shown in Fig. 7 represents the development of the wave form with respect to the Marangoni instability. Note that the wave form moves (rotates) in the direction of the rotation downward toward the cooler bottom. The exposure time was selected such that the motion of the tracer particles appears like streaks. The period of the wave motion was 1.5 s.

Figure 8 shows the number and the slope of the helical structure in loop form (mode 3) for both liquids under consideration. The number of loops as well as their slopes are greater for a fluid having a smaller Pr number (Fig. 8a), and so for a fluid having lower viscosity.

Figure 9 exhibits the structures in lump form that exist in modes 2 and 3. As the temperature gradient increases, the lumps move horizontally as well as spin about their own axis in opposite direction to the cell rotation. The significance of this structure with respect to the mode is not clear and more experiments have to be carried out in this temperature region for clarification.

Owing to photos taken with a long exposure time, one can estimate both the vertical and the azimuthal velocities of moving structures. For instance, Fig. 10 presents the motion of helical structures in loop form (mode 3). The comparison of translations A-A' and B-B' (Fig. 10b) reveals that both vertical and azimuthal velocities are greater for greater z. (Because of the conical shape of the rotating interface, there is, of course, a third component of the velocity vector, viz., a radial one, but it is impossible to see it on this picture.)

C. Flow Configuration

The motion in the rotating liquid-gas zone while heated from above and cooled from below is depicted in Fig. 11. As it was said earlier, the flow in the rotating liquid-gas zone with a free inner surface is significantly influenced by thermocapil-

Mode I   Mode II   Mode III   Mode IV

MODE I   SLOW LAMINAR CONVECTION AT THE INTERFACE
MODE II   WAVE FORM
MODE III WAVE FORM AND HELICAL STRUCTURE
MODE IV   FAST INTERFACIAL FORM

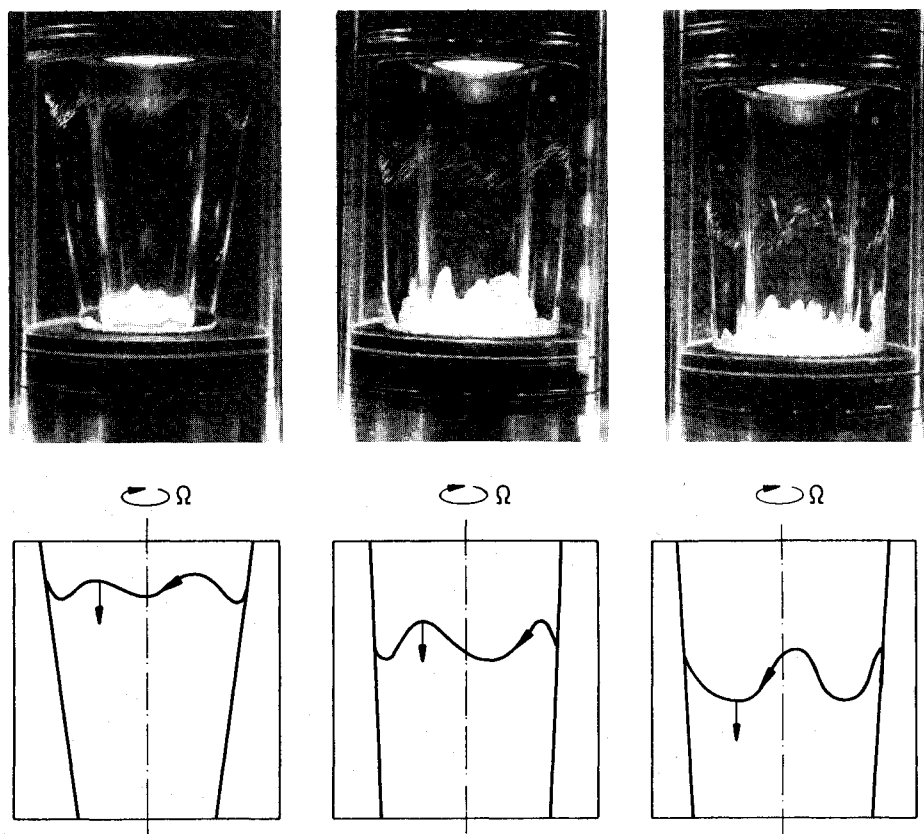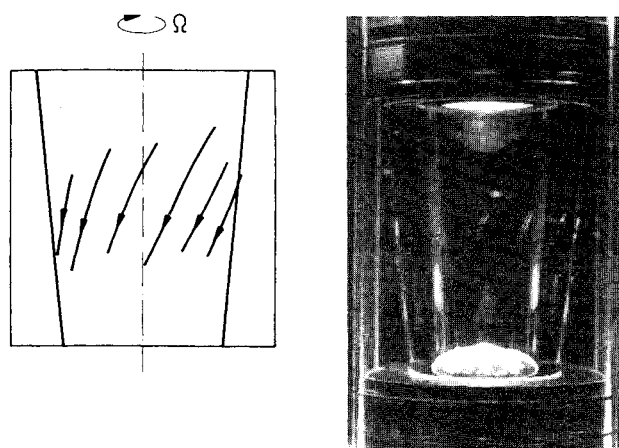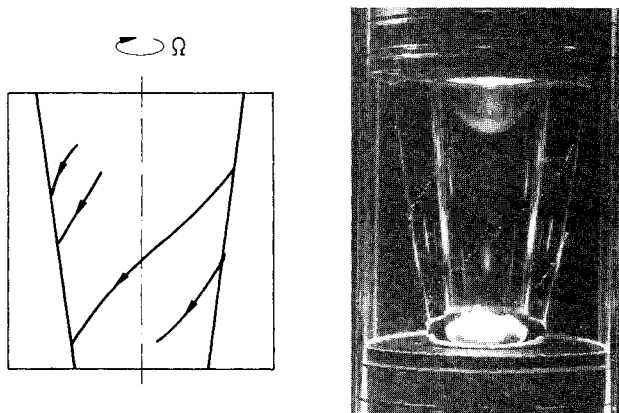Fig. 6 Flow regimes at the interface.

Fig. 7 Development of the wave form in silicone oil AK-5: $Fr = 23$; $\Omega = 104.30$ rad/s (1000 rpm); $Ta = 5.46 \times 10^9$; $E = 2.72 \times 10^{-5}$.

a) $Pr = 6, \Delta T = 6 \text{ K } (Mg = 2.71 \times 10^5)$

b) $Pr = 55, \Delta T = 6 \text{ K } (Mg = 4.85 \times 10^4)$

Fig. 8 Comparison of helical structures in loop form: $Fr = 8$; $\Omega = 62.83$ rad/s (600 rpm).

Fig. 9 Behavior of lump structures in silicone oil AK-0.65: $Pr = 6$; $Fr = 15$; $\Omega = 83.57$ rad/s (800 rpm); $\Delta T = 4.5 \text{ K } (Mg = 2.36 \times 10^5)$

Fig. 10 Velocity profile of a helical structure in loop form in silicone oil AK-5: $Pr = 55$; $Fr = 15$; $\Omega = 62.83$ rad/s (600 rpm); $\Delta T = 20$ K $(Mg = 1.63 \times 10^5)$.

lary convection, gravitational, and centrifugal buoyancy. The motion in the rotating fluid system is composed of four parts: 1) a core motion in the inviscid interior, 2) an Ekman layer on the top and the bottom plates, 3) a sidewall Prandtl-boundary layer, and 4) a thermocapillary boundary layer at the liquid-gas interface. The fourth topological structure is confined to a thin region at the liquid-gas interface. We call this layer the penetration domain of the Marangoni convection.

A fluid particle emerging from the upper Ekman layer moves, concurrent with the rotation, downward toward the bottom Ekman layer and next spirals vertically near to the interface upward to the top Ekman layer. To provide a return flow, a pressure gradient is produced such that the pressure is greater at the bottom than at the top. Because the fluid is weakly stratified, there is no interior radial motion, and on each horizontal plane, the fluid rotates with an angular velocity lower than that of the container.

D. Flow Regime Map

Based on the results presented herein, a thermocapillary flow regime map for a rotating cylindrical liquid-gas interface is presented in Fig. 12.

The onset of the Marangoni convection does not depend on the rotation and the Prandtl number and starts immediately, as mentioned earlier, at any speed of rotation (for $Pr = 6$ and 55) after generation of the temperature gradient (see Fig. 12).

In the case of the smaller Prandtl number ($Pr = 6$), the transition from one flow pattern to the next turns out to be independent of the rotation. Only for a Marangoni number above 25×10^3 does the Marangoni convection at the interface depend slightly on the speed of rotation. In this case, as displayed also in Fig. 12b, the stabilizing effect of the rotation on
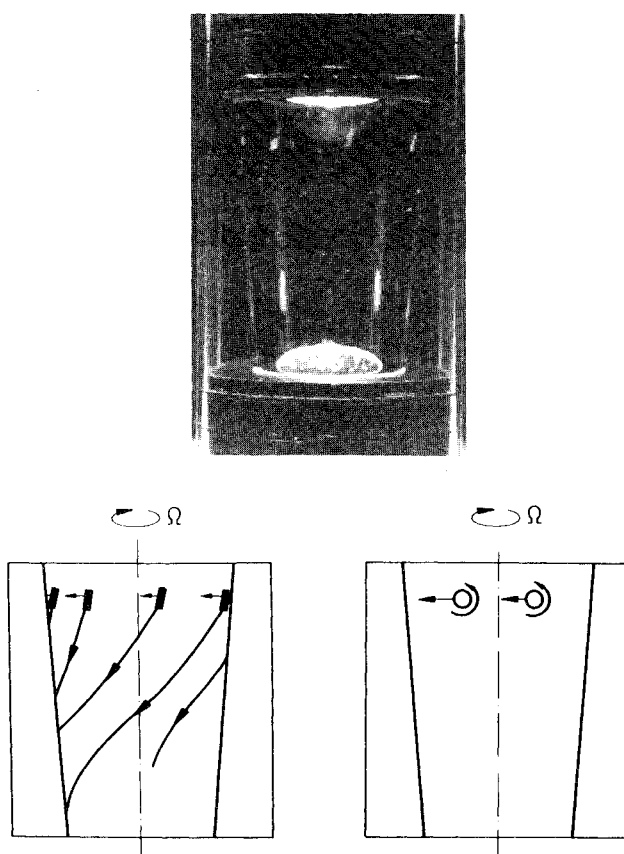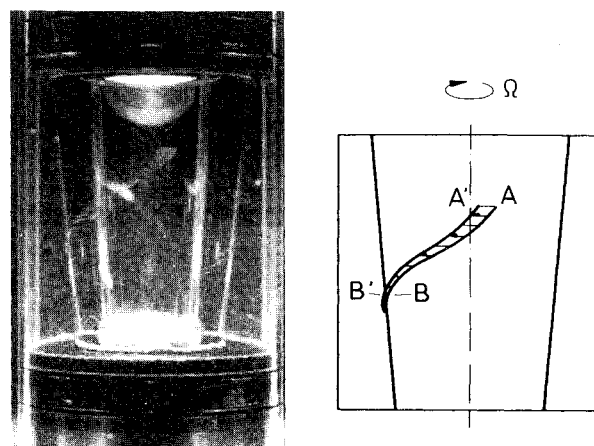
the transition of the one type of flow to another and the effect of the Coriolis force on the flow pattern become observable.

For the liquid-air system having the greater liquid Prandtl number ($Pr = 55$), the transition from one mode to the other depends strongly on the speed of rotation. In other words, the stabilizing effect of rotation on the oscillations is greater than the combined effect of the viscous retardation of the bulk flow and the flowfield due to the surface-temperature variation.

For the smaller Prandtl number (liquid with a lower viscosity), the transition from one mode to another was achieved for smaller Mg numbers and that for all speeds of rotation under consideration.

For AK-5 ($Pr = 55$), the fourth mode was reached only at $\Omega = 600$ rpm and $\Delta T = 63$ K. For safety reasons, the testing
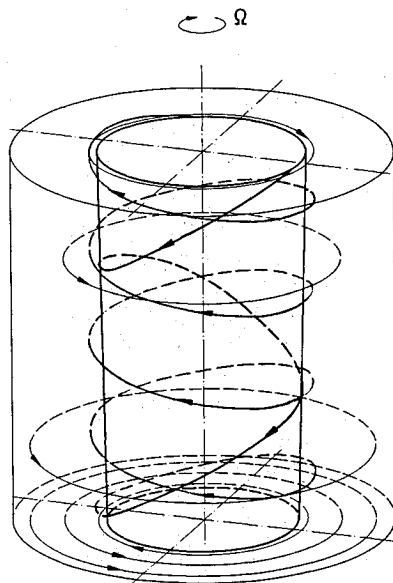
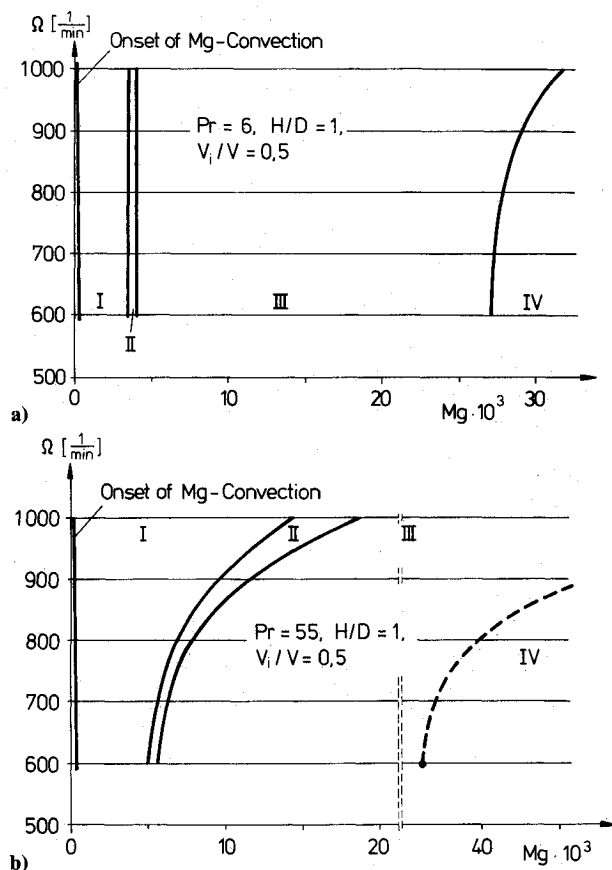**Fig. 11 Flow configuration in the rapidly rotating cylindrical cell.**

Fig. 12 Instability diagram as a function of angular velocity (Froude number) and Marangoni number for different liquids (Prandtl number): a) silicone oil AK-0.65, $Pr = 6$; b) silicone oil AK-5, $Pr = 55$.

stand did not allow larger temperature differences and the fourth mode could not be achieved. Thus, the diagram with respect to the fourth mode (Fig. 12b) has only a hypothetical character (dashed line).

The onset of oscillations cannot be defined by the basic parameter, i.e., the Marangoni number, for a given fluid (fixed Pr) only. The deformability of the liquid-gas interface and the thickness of the thermocapillary boundary layer along the interface are important factors causing oscillations.[17]

The oscillations at the interface are a consequence of a complex coupling between surface deformability, interface velocity, and temperature distribution.[18] According to Ostrach et al.,[19] the coupling tends to induce alternating weak and strong convective heat transfer and a time lag between the surface flow (from the top to the bottom) and the bulk return flow (from the bottom to the top). The effect of the thermal boundary conditions, the interface thermal conditions (the effect of surface heat loss), and the heating method also must be taken into account to characterize the onset of oscillations.

Conclusions

Four different flow regimes at the interface, namely slow laminar mode, wave form, wave form and helical structure in loop form, and fast interfacial form are discovered and classified. A suppressing effect of the rotation on the transition from one mode to the other was observed. The onset of thermocapillary convection does not depend on the rotational speed and the Prandtl number and starts immediately after the temperature gradient is applied. Moreover, the onset of oscillations does not depend on the rotational speed of a fluid having a lower Pr number $Mg_{cr} = 4 \times 10^3$ and depends on Ω for a fluid having higher Pr number $Mg_{cr} = 6 \times 10^3$ and $Mg_{cr} = 15 \times 10^3$ for $\Omega = 600$ and 1000 rpm, respectively. The results show that the thermocapillary flow is confined to a thin layer at the liquid-gas interface for sufficiently small temperature differences.

Acknowledgment

References

[1]Clever, R. M., and Busse, F. H., "Nonlinear Properties of Convection Rolls in a Horizontal Layer Rotating About a Vertical Axis," *Journal of Fluid Mechanics*, Vol. 94, Pt. 4, 1979, pp. 609–627.

[2]Brown, S. N., and Cheng, H. K., "The Response of a Stratified Rapidly Rotating Flow to a Pulsating Topography," *Journal of Fluid Mechanics*, Vol. 177, 1987, pp. 359–379.

[3]Smith, M. K., "Thermocapillary and Centrifugal-Buoyancy-Driven Motion in a Rapidly Rotating Liquid Cylinder," *Journal of Fluid Mechanics*, Vol. 166, 1986, pp. 245–256.

[4]Chun, Ch.-H., and Wuest, W., "Suppression of Temperature Oscillations of Thermal Marangoni Convection in a Floating Zone by Superimposing of Rotating Flows," *Acta Astronautica*, Vol. 9, 1982, pp. 225–230.

[5]Kobayashi, N., "Computer Simulation of the Steady Flow in a Cylindrical Floating Zone Under Low Gravity," *Journal of Crystal Growth*, Vol. 66, 1984, pp. 63–72.

[6]Boubnov, B. M., and Golitsyn, S. S., "Experimental Study of Convective Structures in Rotating Fluids," *Journal of Fluid Mechanics*, Vol. 167, 1986, pp. 503–531.

[7]Barcilon, V., and Pedlosky, J., "On the Steady Motions Produced by a Stable Stratification in a Rapidly Rotating Fluid," *Journal of Fluid Mechanics*, Vol. 29, 1967, pp. 673–690.

[8]Homsy, G. M., and Hudson, J. L., "Centrifugally Driven Thermal Convection in a Rotating Cylinder," *Journal of Fluid Mechanics*, Vol. 35, 1969, pp. 33–52.

[9]Lugt, H. J., and Abboud, M., "Axisymmetric Vortex Breakdown With and Without Temperature Effects in a Container With Rotating Lid," *Journal of Fluid Mechanics*, Vol. 179, 1987, pp. 179–200.

[10]Hunter, C., "The Axisymmetric Flow in a Rotating Annulus Due to a Horizontally Applied Temperature Gradient," *Journal of Fluid Mechanics*, Vol. 27, 1967, pp. 753–778.

[11]Busse, F. H., and Or, A. C., "Convection in a Rotating Cylindrical Annulus: Thermal Rossby Waves," *Journal of Fluid Mechanics*, Vol. 166, 1986, pp. 173–187.

[12]Szymczyk, J. A., and Siekmann, J., " Experimental Investigation of the Thermocapillary Flow Along Cylindrical Interfaces Under Rotation and Low Gravity," *Proceedings of the VIIth European Sym-

posium on Material and Fluid Sciences in Microgravity, ESA-SP 295, Oxford, England, UK, Sept. 1989, pp. 315–320.

[13]Barcilon, V., and Pedlosky, J., "A Unified Linear Theory of Homogeneous and Stratified Rotating Fluids," Journal of Fluid Mechanics, Vol. 29, Pt. 3, 1967, pp. 609–621.

[14]Greenspan, H. P., The Theory of Rotating Fluids, Cambridge University Press, New York, 1969.

[15]Stewartson, K., "On Almost Rigid Rotations," Journal of Fluid Mechanics, Vol. 3, 1957, pp. 17–26.

[16]Barcilon, V., and Pedlosky, J., "Linear Theory of Rotating Stratified Fluid Motions," Journal of Fluid Mechanics, Vol. 29, Pt. 1, 1967, pp. 1–16.

[17]Kamotani, V., and Lee, K. J., "Oscillatory Thermocapillary Flow in a Liquid Column Heated Radiatively by a Ring Heater," Pro-

ceedings of the 7th International Conference Physico Chemical Hydrodynamics, Massachusetts Inst. of Technology, Cambridge, MA, 1989.

[18]Szymczyk, J. A., Chun, Ch.-H., Siekmann, J., and Wozniak, K., "Liquid Crystal Tracers as a Method for Thermocapillary Flow Diagnostics," Archives of Mechanics, Vol. 41, 1989, pp. 351–360.

[19]Ostrach, S., Kamotani, Y., and Lai, C. L., "Oscillatory Thermocapillary Flows," Physico Chemical Hydrodynamics, Vol. 6, 1985, pp. 585–599.

[20]Bauer, H. F., "Marangoni Convection in Rotating Liquid Systems," International Journal for Microgravity Research and Applications, Vol. 2, 1989, pp. 142–157.

Paul Mizera
Associate Editor